NEURO-OPHTHALMOLOGY

Anatomical and functional impairment of the nerve fiber layer in patients with optic nerve head drusen

**Pablo Gili · Patricia Flores-Rodríguez ·
María Dolores Martin-Ríos · Carmen Carrasco Font**

Abstract

Objective To evaluate anatomical and functional impairment of the retinal nerve fiber layer (RNFL) using optical coherence tomography (OCT) and automated perimetry in patients with optic nerve head drusen (ONHD).

Materials and methods Sixty-six eyes (66 patients) were studied with ONHD — confirmed by ultrasound B scan — and 70 eyes (70 subjects) of healthy control subjects. ONHD cases were categorised as visible or hidden. Average RNFL thickness and measurements in terms of the quadrants were analysed using both time-domain optical coherence tomography (TD-OCT) and spectral-domain optical coherence tomography (SD-OCT). Anatomical and visual field alteration of RNFL between visible and hidden ONHD and control groups were compared.

Results Average RNFL thickness in ONHD patients was 94 μm (TD-OCT) and 88 μm (SD-OCT), and in controls 107 μm (TD-OCT) and 96 μm (SD-OCT), with statistically significant differences between both OCTs. All quadrants analysed showed significant differences except the temporal quadrant. The differences were not significant between hidden drusen and controls. Visual field examination in ONHD showed alterations in 56 %. Alterations were greater in visible drusen in relation to non-visible drusen, but there were no significant differences. The association between RNFL defects in superior, inferior and temporal quadrants and visual field defects showed a statistical relation with visible ONHD, but not in hidden ONHD.

Conclusions ONHD caused anatomical and functional damage of the RNFL, with a clear association between the alteration in ONHD and visual field defects in visible drusen cases.

Keywords Optic disk drusen · Optical coherence tomography · Visual field

P. Gili · P. Flores-Rodríguez · C. Carrasco Font
Ophthalmology Unit, Hospital Universitario Fundacion Alcorcon, Madrid, Spain

P. Gili
Health Sciences Faculty, Universidad Europea, Madrid, Spain

P. Flores-Rodríguez
Pontificia Universidad Católica de Valparaíso, Valparaíso, Chile

M. D. Martin-Ríos
Preventative Medicine Unit, Hospital Rey Juan Carlos, Madrid, Spain

P. Gili (✉)
Unidad de Oftalmología, Hospital Universitario Fundación Alcorcón, C/Budapest 1, 28922 Alcorcón, Madrid, España
e-mail: pgili@fhalcorcon.es

Introduction

Optic nerve head drusen (ONHD) are acellular, calcified deposits, which can often be confused with serious pathologies like papiloedema [1]. Its prevalence has been estimated at between 3.4 and 24 per 1,000 of the population, is more common in Caucasians, and has a slight predominance in women. ONHD tend to be asymptomatic, and present bilaterally in 66–85 % of cases without affecting visual acuity [2]. Different methods have been described in ONHD diagnosis: fundus examination [3, 4], fluorescein angiography and autofluorescence [5, 6], scanning laser ophthalmoscope (SLO) [7], computed tomography [8], and recently, optical coherence tomography (OCT) [9]. Since its emergence in the early 1980s, ultrasound has been considered the gold standard in the diagnosis of ONHD [10].

Previous studies have reported the presence of visual field defects (between 71 % and 87 % of cases) [11–13] and reduction of RNFL thickness with OCT in ONHD cases [9, 14, 15].

The aim of the study was to evaluate anatomical and functional impairment of the RNFL using OCT and perimetry

Fig. 1 Topographical orientation adapted from Garway-Heath et al. [20]; relationship between topographic RNFL and visual field pattern
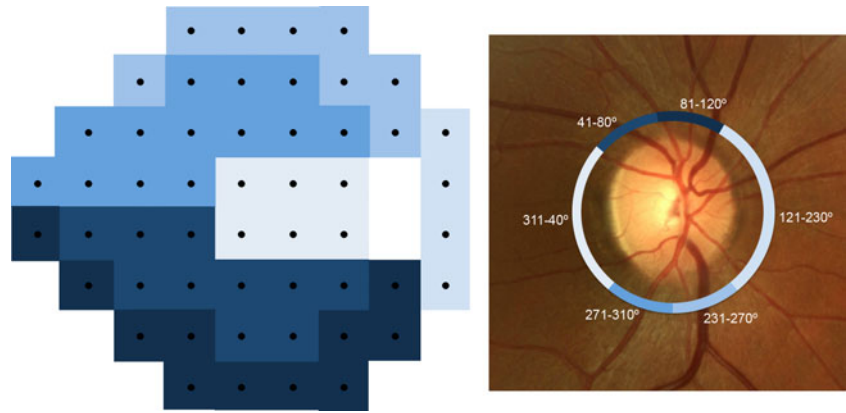
in patients with ONHD, and to analyse the association between RNFL defect location and the type of visual field alteration.

Methods

This study was approved by the ethics committee of the University Hospital Alcorcon Foundation (Spain) and was conducted in accordance with the principles of the Declaration of Helsinki.

A cross-sectional, descriptive study was carried out, which included patients with ONHD and healthy control subjects during the period between March 1 2009 and May 1 2011 in the ophthalmology unit of our hospital.

All patients included in the study underwent measurement of optimal visual acuity (ETDRS logMAR chart at 4 m.), spherocylindrical refraction, anterior segment biomicroscopy, ophthalmoscopic examination under pharmacological mydriasis, two-dimensional ultrasound B (OTI Ophthalmic Technologies Inc.; http://2774.ca.all.biz.), time-domain optical coherence tomography (TD-OCT) using Stratus OCT (version 4.0.7; http://www.meditec.zeiss.com), spectral domain (SD-OCT) using Cirrus OCT (version 5.0.0; http://www.meditec.zeiss.com), and visual field examination with Humphrey Field Analyzer

745 automated perimetry using 24-2 standard program and Sita Fast strategy (Swedish Interactive Threshold Algorithm http://www.meditec.zeiss.com).

Inclusion criteria

Two groups of patients were included: patients with ONHD (visible and hidden) and control subjects.

1) Patients with ONHD: Caucasian patients with ONHD — unilateral or bilateral — were consecutively selected and confirmed in all cases with an ultrasound B scan with a gain of <27 dB (gold standard). ONHD classification was based on the protocol described by Roh et al. [15]:

 – Visible or superficial ONHD: yellowish nodular images, number and size variable, usually elevated papilla and blurry edges
 – Deep or hidden ONHD: papilla usually high and poorly defined edges, no visible nodular images.

2) Control subjects: healthy Caucasian subjects with corrected visual acuity of >0.30 logMAR (Snellen 6/12, 20/40), transparent ocular media, normal intraocular pressure (<21 mmHg) evaluated with Perkins applanation tonometer (http://www.clement-clarke.com/), normal appearance of the optic nerve as indicated by colour fundus photography, OCT, and normal visual field.

Exclusion criteria

The following were excluded from the study:

– Patients for whom certain diagnostic tests could not be performed, as a result of media opacity that prevented fundus photography and/or optical coherence tomography (OCT).
– Patients from whom there was a lack of cooperation for any of the tests.
– Patients who had undergone previous ocular surgeries.

Table 1 Characteristics of the study population

	ONHD ($n=66$)	Control ($n=70$)	P-value
Age (SD)	43.4 (18.8)	41.5 (15.7)	0.518*
Gender (%)			0.331**
Female	60.6 %	68.6 %	
Male	39.4 %	31.4 %	
Spherical equivalent refraction (SD)	−0.66 (3.39)	−0.37 (1.69)	0.697***
AV logMAR	0.02 (0.04)	0.11 (0.19)	<0.0001***

p-value: *Student's t-test; **Chi-square test; ***Mann–Whitney U test

Table 2 Comparison of average RNFL thickness by quadrant between ODE and control subjects with TD-OCT and SD-OCT

	TD-OCT			SD-OCT		
	Control mean (SD)	ODE mean (SD)	*P*-value	Control mean (SD)	ODE mean (SD)	*P*-value
Nasal	72.2 (29.0)	87.2 (19.2)	<0.0001	74.38 (14.2)	66.2 (25.3)	<0.0001
Temporal	73.05 (11.4)	77.2 (29.3)	0.582	64.96 (9.6)	71.0 (32.0)	0.564
Superior	135.31 (20.1)	109.2 (41.7)	<0.0001	121.9 (15.7)	100.3 (43.0)	<0.0001
Inferior	133.63 (17.4)	116.8 (43.1)	0.011	123.98 (16.9)	113.4 (43.5)	0.046
Average thickness	107.01 (10.9)	94.0 (28.7)	0.001	96.33 (10.1)	88.2 (30.9)	0.001

p-value: Student's *t*-test

– Patients with concomitant disease that could affect the optic nerve and/or retinal nerve fiber layer (glaucoma, retinitis pigmentosa, neuropathies, macular diseases, vascular occlusions, chiasmatic tumors, and others).

Optical coherence tomography

All OCT examinations were performed by one operator (P.F.) on the same day and within a maximum time range of 1 h between the two models used. The only OCT images included were those with signal quality >7, with centred position, and those with correct determination of the layer border of the RNFL. Tomographic examination protocols used were: fast RNFL thickness with Stratus OCT, and optic disc cube 200×200 protocol with Cirrus OCT. Average RNFL thickness and measurements in terms of quadrants were analysed, with data obtained automatically by both types of equipment.

Automated perimetry

Humphrey Field Analyzer 745 automated perimetry (24-2 standard program) and Sita Fast strategy were used for the study of functional impairment. Selection of visual fields in the study were made in accordance with the following "Collaborative Normal-Tension Glaucoma Study Group" [16] reliability criteria: with a loss of fixation and false positive errors ≤15 % and false negative errors ≤30 %. At least two visual field examinations were required in order to define a perimetry as pathological, with a default similarity between the first and second. One single visual field per eye was chosen for the analysis.

Normality criteria for visual field were in accordance with previous studies on patients with ONHD [17, 18]:

a) Normal visual field: mean deviation (MD) less than −2.0 dB

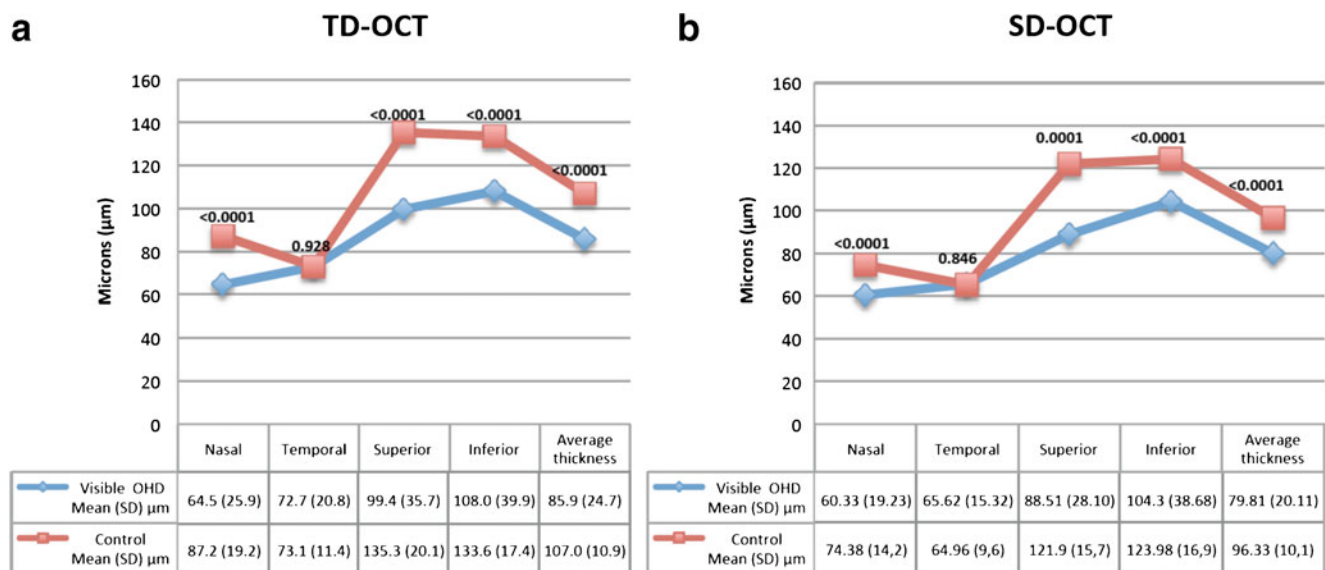b) Abnormal visual field: Must meet at least one of the three criteria:

Fig. 2 Measurement of average RNFL thickness and by quadrant between visible ONHD and controls with TD-OCT (**a**) and SD-OCT (**b**)
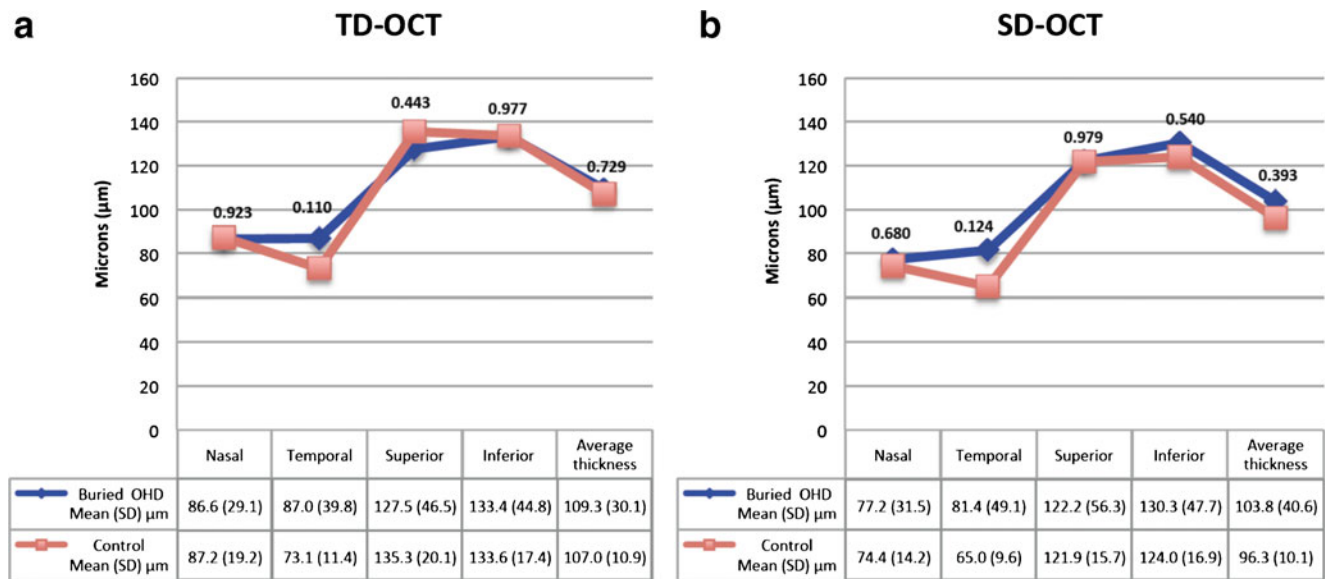
Fig. 3 Measurement of average RNFL thickness and by quadrant between hidden ONHD and controls with TD-OCT (**a**) and SD-OCT (**b**)

- Glaucoma hemifield test outside normal limits (PHG).
- Standard deviation model (PSD) with probability lower than 5 %.
- Three or more points on the deviation pattern graph in a hemifield (lower or higher) with probability lower than 5 %, one of which must have a probability level of at least 1 % [19].

Topographical orientation was adapted from Garway-Heath et al. [20] (Fig. 1) in order to observe the association between different regions of the visual field with an optical disc sector in OCT. In addition, enlargement of the blind spot was added as a defect that expands the physiological edges of a normal one.

The abnormality criteria mentioned above were followed in order to be able to consider actual visual field defects within one or more of the seven visual field sectors [17, 18]. The

frequency of visual field normality, visual field indices of mean deviation (MD), and average standard deviation (PSD) were analysed, along with the association between the location of the defect in the RNFL thickness by quadrant in OCT and visual field pattern found.

Statistical analysis

In the descriptive analysis, quantitative variables are expressed in mean and standard deviation (SD) for 95 % confidence intervals. Mean comparison was performed using the Student's t-test and the nonparametric equivalent — the Mann–Whitney U test. Qualitative variables are represented in frequency distributions. Pearson's Chi-square test ($\times 2$) or Fisher's exact test were used in order to study the association between these variables, in the event that more than 25 % were under 5. Random selection of one eye for inclusion in the study was

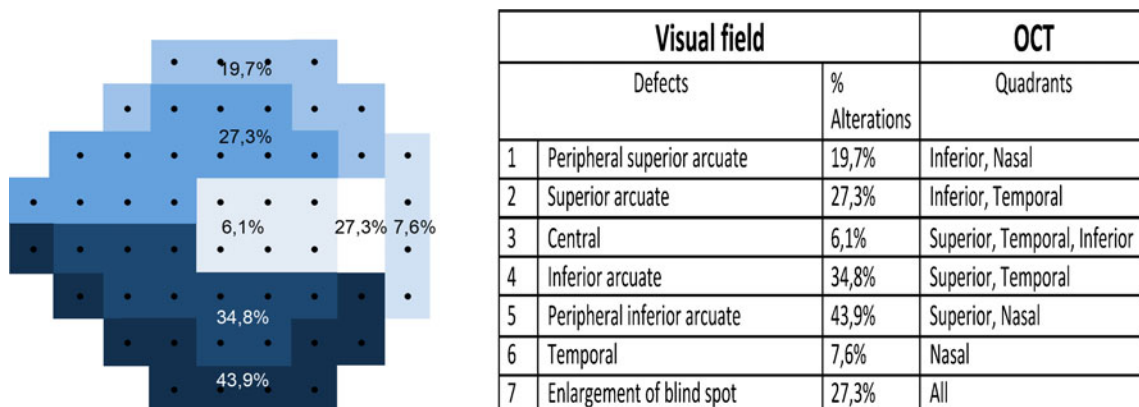|	Visual field		OCT
	Defects	% Alterations	Quadrants
1	Peripheral superior arcuate	19,7%	Inferior, Nasal
2	Superior arcuate	27,3%	Inferior, Temporal
3	Central	6,1%	Superior, Temporal, Inferior
4	Inferior arcuate	34,8%	Superior, Temporal
5	Peripheral inferior arcuate	43,9%	Superior, Nasal
6	Temporal	7,6%	Nasal
7	Enlargement of blind spot	27,3%	All

Fig. 4 Patterns of visual field defects in patients with ONHD shown as a percentage and the relation with optical coherence tomography (OCT)

Table 3 Association between the defect in RNFL thickness in OCT by quadrant and visual field pattern type affected in visible ONHD

Visible ONHD	Nasal				Temporal				Superior				Inferior			
	1	P-value	2	P-value	1	P-value	2	P-value	1	P-value	2	P-value	1	P-value	2	P-value
Peripheral superior arcuate	40 %	0.073*	40 %	0.073*	–	–	–	–	–	–	–	–	50 %	0.001*	50 %	0.001*
Superior arcuate	–	–	–	–	100 %	<0.0001	100 %	0.006*	–	–	70 %	<0.0001	67 %	<0.0001	67 %	<0.0001
Peripheral inferior arcuate	47 %	0.988	53 %	0.512	–	–	–	–	76 %	<0.0001	70 %	<0.0001	–	–	–	–
Inferior arcuate	–	–	–	–	83 %	0.021	100 %	0.015*	67 %	<0.0001	56 %	0.001	–	–	–	–
Central	–	–	–	–	50 %	0.006*	75 %	0.001*	14 %	0.345*	15 %	0.279*	22 %	0.025*	22 %	0.025*
Temporal	7 %	1.00*	13 %	0.275*	–	–	–	–	–	–	–	–	–	–	–	–
Enlargement of blind spot	54 %	0.12*	47 %	0.074*	100 %	<0.0001	100 %	0.004	48 %	0.005	44 %	0.001	61 %	<0.0001	61 %	<0.0001

1 = TD-OCT; 2 = SD-OCT; *p*-value: Chi-square test

*Fisher's exact test

made in all patients with bilateral pathology of ONHD and in healthy subjects.

A significance level of 0.05 was established. Statistical analysis was performed using SPSS program for Windows (version 15.0.1, http://www.01.ibm.com/software/analytics/spss/).

Results

One hundred and thirty-six eyes of 136 Caucasian patients were studied: 66 eyes with ONHD confirmed by ultrasound B and 70 eyes of healthy subjects.

Fifty-nine ONHD patients had bilateral drusen (89 %) and seven patients unilateral (11 %). We analised the type of drusen; we found 38 visible drusen and 28 hidden drusen. Three patients had angioid streaks, one with pseudoxanthoma elasticum. Six of the ONHD patients group included in the study had a family history of ONHD. None of them had history of concomitant ocular pathology previously, considered in the exclusion criteria (retinitis, membrane neovascular, glaucoma, vascular occlusion, etc.).

Table 1 shows the characteristics of the study population in both diagnostic groups, without significant differences, except for diminished visual acuity measurement in the ONHD group in relation to controls ($p<0.0001$).

Measurement of RNFL thickness showed greater reduction in ONHD patients in relation to controls (Table 2), and a statistical significance in patients with visible ONHD in all quadrants except for temporal quadrant, with both types of equipment (Fig. 2). In contrast, hidden ONHD showed no statistical significant differences in average thickness in any quadrants in relation to controls, with both types of tomography ($p<0.005$) (Fig. 3).

Fifty-six per cent of these cases showed visual field alteration, more often visible in ONHD patients (58 %) than in hidden ONHD patients (52 %), ($p=0.640$). Patterns of visual field defects in ONHD were as follows: peripheral inferior arcuate 43.9 % ($n=29$), inferior arcuate 34.8 % ($n=23$), enlargement of blind spot and superior arcuate 27.3 % ($n=18$), peripheral superior arcuate 19.7 % ($n=13$); temporal defect 7.6 % ($n=5$), and central defect 6.1 % ($n=4$) (Fig. 4).

The quantitative analysis with MD and PSD indices in ONHD values showed −5.12 (7.2) dB and 3.9 (3.0) dB respectively, with greater defect in visible ONHD in relation to hidden ONHD, MD −5.3 (7.8) and −4.8 (6.1) dB, and PSD 3.9 (3.1) and 3.8 (2.9), with no statistical significant differences ($p=0.514$ and $p=0.128$).

Results of the association between the location of the defect in RNFL thickness by sector (with TD-OCT and SD-OCT) and visual field pattern type affected were statistically significant in visible ONHD, but not in hidden ONHD, with both OCTs (Tables 3 and 4).

Table 4 Association between the defect in RNFL thickness in OCT by quadrant and visual field pattern type affected in hidden ONHD

Buried ONHD	Nasal				Temporal				Superior				Inferior			
	1	P-value	2	P-value	1	P-value	2	P-value	1	P-value	2	P-value	1	P-value	2	P-value
Peripheral superior arcuate	0 %	1.00*	0 %	1.00*									0 %	0.539*	0 %	1*
Superior arcuate					0 %	1.00*	0 %	1.00*					17 %	1*	20 %	1*
Peripheral inferior arcuate	25 %	1.00*	25 %	1.00*					57 %	0.363	50 %	0.657*				
Inferior arcuate					50 %	0.526*	50 %	0.526*	57 %	0.137*	50 %	0.182*				
Central					0 %	1.00*	0 %	1.00*	0 %	1*	0 %	1*	0 %	1*	0 %	1*
Temporal	0 %	1.00*	0 %	1.00*												
Enlargement of blind spot	0 %	0.539*	0 %	0.539*	0 %	1.00*	0 %	1.00*	0 %	0.124*	13 %	0.369	17 %	1*	20 %	1*

1 = TD-OCT; 2 = SD-OCT; *p*-value: Chi-square test
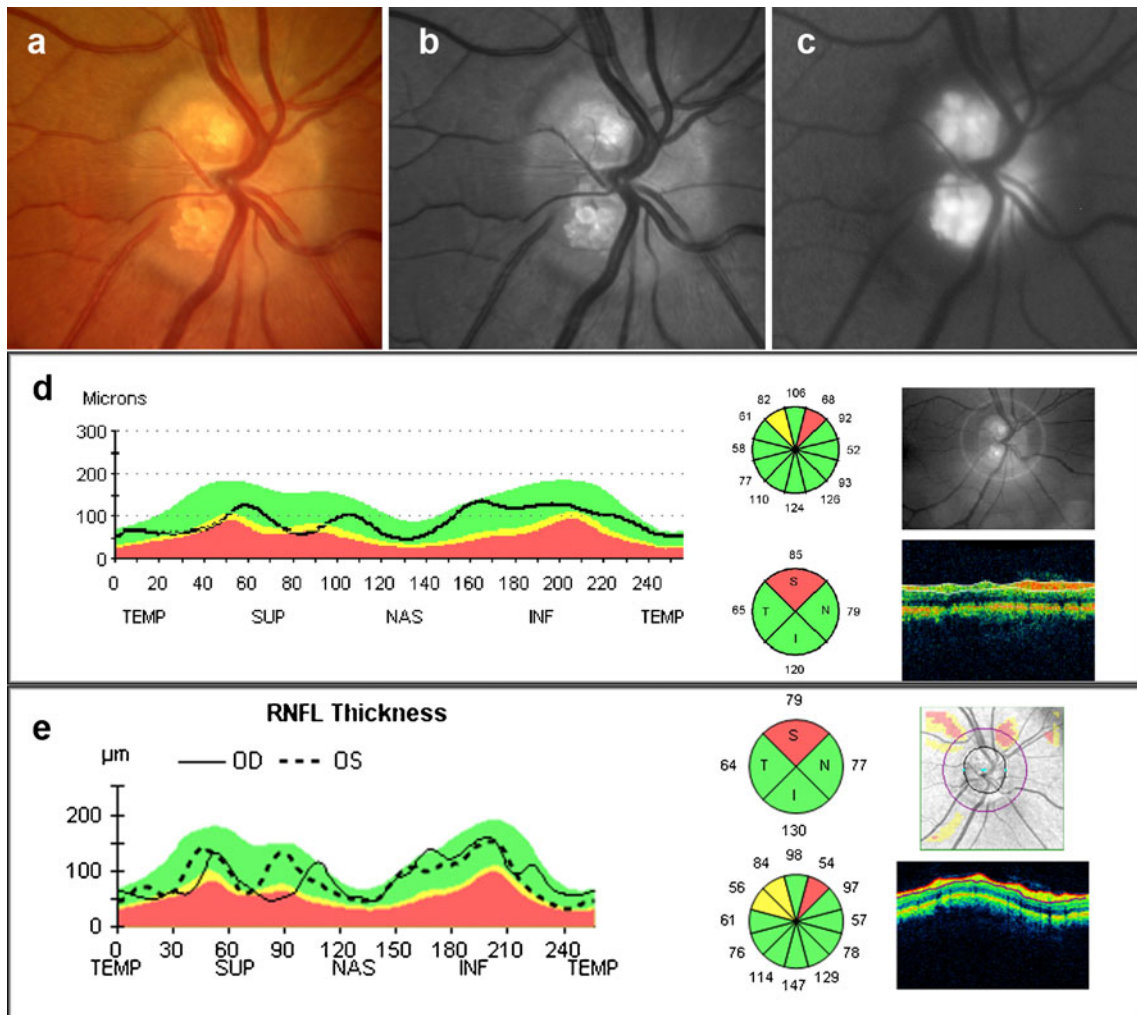
*Fisher's exact test

Fig. 5 Visible optic nerve head drusen. **a** Color fundus photography 20°. **b** Red-free photography. **c** Fundus autofluorescence. **d** Retinal fiber nerve layer: time-domain optical coherence tomography (TD-OCT). **e** Retinal fiber nerve layer: spectral-domain optical coherence tomography (SD-OCT)

Discussion

The reduction of RNFL thickness in patients with ONHD was the subject of interest before 1957 in studies conducted by Lansche [21] and Mustonen & Nieminen [22] with fundus photography (green filter). However, interpretation with this conventional technique can often be complicated due to the presence of media opacity [22]. Optical coherence tomography proved useful in quantifying the loss of RNFL thickness in ONHD cases with regard to healthy subjects [9, 14, 15]. Previous studies, such as the one conducted by Roh et al. [15] on 23 eyes with ONHD, show that the greater the visibility of ONHD (Fig. 5), the greater the reduction of RNFL thickness in the superior and inferior quadrants with TD-OCT. In this study, RNFL thickness measured with TD-OCT and SD-OCT showed greater reduction in the visible ONHD group compared with the controls in all quadrants except for the temporal, probably because it is less common to find ONHD in this quadrant, therefore contributing to the pathogenic theory, which suggests that the presence of ONHD produces compression of the optic disc and leads to a loss of RNFL in OCT [15]. In contrast, the difference in thickness between hidden ONHD and controls did not prove to be significant in any quadrants or averages. Katz [13] studied 58 eyes with hidden ONHD using the same OCT technology, and also failed to find impairment of RNFL thickness.

Visual field defects in patients with ONHD have been described in 71 % to 81 % of cases. These defects have shown to increase in size as the ONHD become more visible over the years [11–15, 23]. One of the most classical theories is that these calcium accumulations produce compression of the optic disc close to the axons of the ganglion cells, causing them to die, leading to visual field loss [24]. However, some authors have reported that there is not necessarily a correlation between the location of ONHD and the location of the visual field defect [25]. As mentioned in the study by Walsh & Hoyt [26], if ONHD are located in the deep zones adjacent to the cribriform plate, visual field defects are caused. There are various studies that have found a higher percentage of abnormal visual fields in visible ONHD patients in relation to hidden ONHD patients, such as those by Savino [11] (86 % and 62 %); Mustonen [27] (75 % and 48 %); and Wilkins [12] (73 % and 36 %). In our study, a higher percentage of abnormal visual fields were found in visible ONHD patients (58 %) in relation to hidden ONHD (52 %), but with no significant differences. Moreover, the quantitative study of functional damage with MD and PSD indices showed that visible ONHD have greater visual field damage than hidden ONHD, which can be likened to results found by Wilkins [12]. Discrepancy between our results and those shown by other authors may be due to the selection criteria and definition of significant visual field defects. We have used a series of quantitative criteria adopted by a consensus of experts specialized in the analyses

of patients' visual field [16]. Our purpose was to diminish the weaknesses displayed by the use of subjective criteria in previous studies [11, 12, 27].

The association between the location of the defect in RNFL thickness and location of visual field defects has been studied in patients with glaucoma [28] and some optic neuropathies [29]. Roh et al. [15], in a study of 23 eyes with ONHD, found that OCT may be a good indicator of sectors with RNFL thickness reduction, which seems to correspond with visual field defects. However, it does not study the relationship between the types of visual field pattern found. The most common visual field patterns found are the enlargement of the blind spot and arcuate defects [11, 27, 30–32]. The study by Guerrero [33] of 20 patients with ONHD, evaluated the relationship between the location of RNFL thickness and the visual field pattern type. We concur with Guerrero, in the sense that association is statistically significant in superior, inferior, and temporal quadrants, in visible ONHD cases but not hidden ONHD ones. However, in contrast to this author, a statistically significant association in the nasal quadrant was not found. Lack of a precise topographic correlation may be due to several factors: subjectivity of the visual field, variability in the interpretation of visual field defects, and lack of exact topographic correspondence between optic disc, RFNL, and visual field [33, 34].

In conclusion, ONHD caused anatomical and functional damage of the RNFL, with a clear association between impairment in OCT and the type of visual field defects found in visible drusen cases, but this finding was not observed in hidden drusen cases.

References

1. Sadun AA, Wang MY (2011) Abnormalities of the optic disc. Handb Clin Neurol 102:117–157
2. Auw-Haedrich C, Staubach F, Witschel H (2002) Optic disk drusen. Surv Ophthalmol 47:515–532
3. Lam BL, Morais CG Jr, Pasol J (2008) Drusen of the optic disc. Curr Neurol Neurosci Rep 8:404–408
4. Gili P, Flores-Rodríguez P, Yangüela J, Orduña-Azcona J, Martín-Ríos MD (2013) Evaluation of optic disc size in patients with optic nerve head drusen with fundus photography. J Optom 6:75–79
5. Mustonen E, Nieminen H (1982) Optic disc drusen—a photographic study. I. Autofluorescence pictures and fluorescein angiography. Acta Ophthalmol (Copenh) 60:849–858
6. Kelley JS (1974) Autofluorescence of drusen of the optic nerve head. Arch Ophthalmol 92:263–264
7. Haynes RJ, Manivannnan A, Walker S, Sharp PF, Forrester JV (1997) Imaging of optic nerve head drusen with the scanning laser ophthalmoscope. Br J Ophthalmol 81:654–657

8. Bec P, Adam P, Mathis A, Alberge Y, Roulleau J, Arne JL (1984) Optic nerve head drusen. High-resolution computed tomographic approach. Arch Ophthalmol 102:680–682

9. Flores-Rodríguez P, Gili P, Martín-Ríos MD (2012) Sensitivity and specificity of time-domain and spectral-domain optical coherence tomography in differentiating optic nerve head drusen and optic disc oedema. Ophthal Physiol Opt 32:213–221

10. Atta HR (1988) Imaging of the optic nerve with standardised echography. Eye 2:358–366

11. Savino PJ, Glaser JS, Rosenberg MA (1979) A clinical analysis of pseudopapilledema: II, visual field defects. Arch Ophthalmol 97:71–75

12. Wilkins JM, Pomeranz HD (2004) Visual manifestations of visible and buried optic disc drusen. J Neuroophthalmol 24:125–129

13. Katz BJ, Pomeranz HD (2006) Visual field defects and retinal nerve fiber layer defects in eyes with buried optic nerve drusen. Am J Ophthalmol 141:248–253

14. Menke MN, Feke GT, Trempe CL (2005) OCT measurements in patients with optic disc edema. Invest Ophthalmol Vis Sci 46:3807–3811

15. Roh S, Noecker RJ, Schuman J, Hedges TR, Weiter JJ, Mattox C (1998) Effect of Optic nerve head drusen on nerve fiber layer thickness. Ophthalmology 105:878–885

16. Collaborative Normal-Tension Glaucoma Study Group (1998) Comparison of glaucomatous progression between untreated patients with normal-tension glaucoma and patients with therapeutically reduced intraocular pressures. Am J Ophthalmol 126:487–497

17. Budenz DL, Rhee P, Feuer WJ, McSoley J, Johnson CA, Anderson DR (2002) Comparison of glaucomatous visual field defects using standard full threshold and Swedish interactive threshold algorithms. Arch Ophthalmol 120:1136–1141

18. Katz J, Sommer A, Gaasterland DE, Anderson DR (1991) Comparison of analytic algorithms for detecting glaucomatous visual field loss. Arch Ophthalmol 109:1684–1689

19. Hodapp E, Parrish RK II, Anderson DR (1993) Clinical decisions in glaucoma. Mosby, St Louis, pp 52–61

20. Garway-Heath DF, Poinoosawmy D, Fitzke FW, Hitchings RA (2000) Mapping the visual field to the optic disc in normal tension glaucoma eyes. Ophthalmology 107:1809–1815

21. Lansche RK, Rucker CW (1957) Progression of defects in visual fields produced by hyaline bodies in optic disks. AMA Arch Ophthalmol 58:115–121

22. Mustonen E, Nieminen H (1982) Optic disc drusen—a photographic study. II. Retinal nerve fibre layer photography. Acta Ophthalmol (Copenh) 60:859–872

23. Grippo TM, Shihadeh WA, Schargus M, Gramer E, Tello C, Liebmann JM, Ritch R (2008) Optic nerve head drusen and visual field loss in normotensive and hypertensive eyes. J Glaucoma 17:100–104

24. Wirtschafter JD (1983) Optic nerve axons and acquired alterations in the appearance of the optic disc. Trans Am Ophthalmol Soc 81:1034–1091

25. Pollack IP, Becker B (1962) Hyaline bodies (drusen) of the optic nerve. Am J Ophthalmol 54:651–654

26. Walsh FB (1957) Clinical neuro-ophthalmology. Williams& Wilkins, Baltimore, p 349

27. Mustonen E (1983) Pseudopapilloedema with and without verified optic disc drusen: a clinical analysis, II—visual fields. Acta Ophthalmol 61:1057–1066

28. Schuman JS (2008) Spectral domain optical coherence tomography for glaucoma (an AOS thesis). Trans Am Ophthalmol Soc 106:426–458

29. El Beltagi TA, Bowd C, Boden C, Amini P, Sample PA, Zangwill LM, Weinreb RN (2003) Retinal nerve fiber layer thickness measured with optical coherence tomography is related to visual function in glaucomatous eyes. Ophthalmology 110:2185–2191

30. Lorentzen SE (1966) Drusen of the optic disk: a clinical and genetic study. Acta Ophthalmol 90(Suppl):1–180

31. Erkkilä H (1975) Clinical appearance of optic disc drusen in childhood. Albrecht Von Graefes Arch Klin Exp Ophthalmol 193:1–18

32. Hoover DL, Robb RM, Petersen RA (1988) Optic disc drusen in children. J Pediatr Ophthalmol Strabismus 25:191–195

33. Guerrero L (2010) Estudio de la cuantificación de la capa de fibras nerviosas de la retina mediante tomografía de coherencia óptica de dominio espectral (Cirrus) y de dominio de tiempo (Stratus) en pacientes con drusas del nervio óptico (PhD thesis). Universidad de Alcalá. Madrid

34. Ferreras A, Pablo LE, Garway-Heath DF, Fogagnolo P, Garcia-Feijoo J (2008) Mapping standard automated perimetry to the peripapillary retinal nerve fiber layer in glaucoma. Invest Ophthalmol Vis Sci 49:3018–3025